

## Lattice Boltzmann scheme for two-dimensional magnetohydrodynamics

S. Succi

*IBM European Center for Scientific and Engineering Computing, via Giorgione 159, I-00147 Roma, Italy*

M. Vergassola

*Dipartimento di Fisica, Università "La Sapienza," Piazzale Aldo Moro 2, I-00185 Roma, Italy*

R. Benzi

*Dipartimento di Fisica, Università "Tor Vergata," via Enrico Carnevale, I-00173 Roma, Italy*

(Received 16 May 1990)

It is shown that the lattice Boltzmann equation arising from the basic lattice-gas scheme for Navier-Stokes equations can be extended in such a way as to include the effects of a two-dimensional magnetic field. This offers the possibility of developing new computational schemes for the efficient simulation of incompressible magnetohydrodynamic flows.

Lattice gases (LG's) are a special class of cellular automata (CA) specifically designed to simulate fluid flows by purely Boolean means.<sup>1-3</sup> Although, to date, the major focus of LG research has been placed on the simulation of the Navier-Stokes (NS) equations, it was soon recognized that, with the appropriate modifications, the basic CA scheme for NS equations can be extended in such a way as to describe other types of fluid-related applications. Magnetohydrodynamics (MHD) is such an extension. The first MHD automaton was proposed by Montgomery and Doolen.<sup>4</sup> These authors insisted that, due to the nonlocal nature of the Lorentz force  $\mathbf{J} \times \mathbf{B}$ , the MHD automaton should necessarily be assisted by a finite-differencing stage, yielding the current in terms of derivatives of the vector potential. This leads to a sort of hybrid scheme. However, Chen and Matthaus<sup>5</sup> pointed out that the nonlocality of the Lorentz force is only apparent, in the sense that, by treating the magnetic field  $\mathbf{B}$  on the same footing as the fluid current  $\mathbf{J}$ , the quantity  $\mathbf{J} \times \mathbf{B}$  can be computed locally along the particle trajectory, precisely the same way as one does for the nonlinear term  $(\mathbf{v} \cdot \nabla)\mathbf{v}$  of the NS equation. The need of treating  $\mathbf{B}$  on the same footing as  $\mathbf{J}$ , i.e., like a particle current, leads to a cellular automaton with  $(6)(2)=12$  Boolean variables per node,  $n_{ij}$ , with the index  $i=1,6$  referring to the six possible speeds (we are considering the six-bit Frisch-Hasslacher-Pomeau two-dimensional CA) and  $j=1,2$  to  $\mathbf{J}$  and  $\mathbf{B}$ , respectively. In this Brief Report we show that by introducing the kinetic counterpart of Boolean automata [the lattice Boltzmann (LB) formulation], a suitable MHD-LB scheme can be found that allows the simulation of two-dimensional MHD flows at a computational cost much smaller than the two schemes previously mentioned.

The present work is entirely developed within the framework of the theory of the lattice Boltzmann equation (LBE).<sup>6</sup> A full account on this theory is given in Refs. 7 and 8; here we shall content ourselves with a rapid survey on the most important issues.

The LBE is a set of explicit finite-difference equations

for the evolution of the mean populations  $N_i$  associated with the occupation numbers  $n_i$  ( $n_i=0,1$ ) of the corresponding Boolean automaton. In general, we shall refer to these mean populations as "mesoscopic fields," in that they result from an ensemble average over the microscopic dynamics, even though not all of them are necessarily relevant to the hydrodynamic scale. For the case of the face-centered-hypercubic (fchc) lattice,<sup>3</sup> the LBE takes the following form:

$$S_i N_i \equiv N_i(\mathbf{x} + \hat{\mathbf{c}}_i, t + 1) - N_i(\mathbf{x}, t) = \Omega_{ij}(N_j - N_j^{\text{eq}}), \quad (1)$$

where  $\hat{\mathbf{c}}_i$ ,  $i=1,24$ , are the unit vectors along the directions of the fchc lattice and  $\Omega_{ij}$  is the collision matrix expressing the change in the  $i$ th population induced by a unit change in the  $j$ th population. Finally,  $N_i^{\text{eq}}$  represents the equilibrium distribution function (EDF) resulting from the underlying lattice-gas dynamics. Under a quite general set of conditions on the collision operator, the EDF takes the form

$$N_i^{\text{eq}} = d [1 + 2c_{i\alpha} v_\alpha + G(\rho) Q_{i\alpha\beta} v_\alpha v_\beta] + O(v^2), \quad \alpha, \beta = 1, \dots, 4, \quad i = 1, 24 \quad (2)$$

where  $d$  is the average density per velocity state and  $Q_{i\alpha\beta} = c_{i\alpha} c_{i\beta} - \frac{1}{2} \delta_{\alpha\beta}$ . A deep insight in the dynamics of the LBE can be gained by inspecting the spectral properties of the collision matrix  $\Omega_{ij}$ . It is important to note that the matrix need not be associated with any specific underlying cellular-automaton dynamics. The prescription of  $\Omega$  is, in fact, largely free except for constraints of mass and momentum conservation and the symmetry requirement that  $\Omega_{ij}$  only depends on the cosine between  $\hat{\mathbf{c}}_i$  and  $\hat{\mathbf{c}}_j$ . Owing to this property, the matrix is symmetric and cyclic, so that the spectrum and the corresponding eigenvectors can be computed exactly. One finds four distinct real eigenvalues ( $0$ ,  $\lambda$ ,  $\sigma$ , and  $\tau$ ) with multiplicities 5, 9, 8, and 2, respectively. The five null eigenvalues are associated with the collision invariants, i.e., particle

number and linear momentum, and the corresponding eigenvectors are given by  $1_i$  and  $c_{i\alpha}$ . By projecting the mesoscopic fields  $N_i$ , to be intended here as a 24-dimensional vector, over  $1_i$  and  $c_{i\alpha}$ , one generates five hydrodynamic fields:  $\rho = \sum_i N_i$  and  $J_\alpha = \sum_i N_i c_{i\alpha}$ , which correspond to the fluid density and current density, respectively. As in continuum kinetic theory, the nonzero eigenvalues are associated with transport properties. The eigenvalue  $\lambda$  controls the momentum diffusivity  $\nu$ , which ultimately determines the Reynolds number of the flow  $Re = vL/\nu$ ,  $v$  and  $L$  being typical velocity and length scales. The corresponding set of eigenvectors is given by  $Q_{i\alpha\beta}$ , which, in view of the symmetric and traceless nature of  $Q_{i\alpha\beta}$ , yields nine independent vectors, in accordance with the multiplicity of  $\lambda$ . The projection over  $Q_{i\alpha\beta}$  yields the stress tensor  $S_{\alpha\beta}$ . The eigenvalues  $\sigma$  and  $\tau$  are somehow peculiar to the LBE, in the sense that they describe the relaxation towards equilibrium of a special class of mesoscopic fields which have no direct physical meaning on the hydrodynamic level. In fact, it can be proved<sup>7</sup> that their activity is confined to the short-scale dynamics, at wavelengths comparable to the lattice pitch. At these scales the local Knudsen number is  $O(1)$ , so that the Chapman-Enskog expansion is untenable, which means that these fields take part in the dynamics, but cannot be promoted from the mesoscopic to the hydrodynamical scale; hence we have attached the label ‘‘ghost fields’’ to them to indicate that their activity is confined to small, nonhydrodynamic scales. As a result, the macrodynamical behavior of LBE is represented by the following set of equations:

$$\begin{aligned} \partial_t \rho + \partial_\alpha J_\alpha &= 0, \\ \partial_t J_\alpha + \partial_\alpha(\rho/2) + \partial_\beta S_{\alpha\beta} + \frac{1}{6} \partial_\beta \partial_\beta J_\alpha &= 0, \\ \partial_t S_{\alpha\beta} + \frac{1}{3} [\partial_\alpha J_\beta + \partial_\beta J_\alpha - \frac{1}{2} (\partial_\gamma J_\gamma) \delta_{\alpha\beta}] &= \lambda (S_{\alpha\beta} - S_{\alpha\beta}^{\text{eq}}), \end{aligned} \quad (3)$$

where

$$S_{\alpha\beta}^{\text{eq}} = \rho g(\rho) \left[ v_\alpha v_\beta - \frac{v^2}{4} \delta_{\alpha\beta} \right], \quad (4)$$

and  $g(\rho)$  is the usual factor resulting from the breaking of Galilean invariance in a lattice.<sup>1</sup> Furthermore, it can be proved<sup>7</sup> that, in the adiabatic limit  $\partial_t/\lambda \ll 1$ , these equations converge to the NS equations.

The original four-dimensional LBE can be projected down to three or two dimensions with a possible corresponding increasing reduction of the number of independent fields. In three dimensions, by imposing the appropriate degeneracies, one is left with only 18 populations and  $J_4 = 0$ . It can be shown<sup>1</sup> that in the absence of these degeneracies  $J_4$  behaves like a passive scalar transported by the three-dimensional flow. In two dimensions, one can impose some additional degeneracies, leaving only nine independent populations and  $J_3 = 0$ . We will now exhibit a  $2 + \frac{1}{2}$  model (two space coordinates plus three velocity components) in which the degrees of freedom released by relaxing the degeneracies can be exploited to simulate the presence of a two-dimensional (2D) magnetic field. To this purpose, the 2D MHD equations are most conveniently recast in terms of evolution equa-

tions for a pair of stream functions  $\phi$  and  $\psi$  associated with the magnetic field  $\mathbf{B} = \hat{\mathbf{z}} \times \partial \phi$  and the flow velocity  $\mathbf{v} = \hat{\mathbf{z}} \times \partial \psi$ ,  $\hat{\mathbf{z}}$  being the unit vector along the third ignorable coordinate:

$$\partial_t \phi + (\mathbf{v} \cdot \partial) \phi = \chi \Delta \phi, \quad (5)$$

$$\partial_t (\Delta \psi) + (\mathbf{v} \cdot \partial) (\Delta \psi) = (\mathbf{B} \cdot \partial) (\Delta \phi) + \eta \Delta (\Delta \psi). \quad (6)$$

Let us now see how these equations can be deduced from the full set of Eqs. (3). As anticipated, we have only two spatial coordinates,  $x$  and  $y$ , but three current components. The macrodynamical equations for  $J_z$ ,  $S_{xz}$ , and  $S_{yz}$  take the following explicit form:

$$\begin{aligned} \partial_t J_z + \partial_x S_{xz} + \partial_y S_{yz} &= 0, \\ \partial_t S_{xz} + \frac{1}{3} \partial_x J_z &= \lambda [S_{xz} - \rho g(\rho) v_x v_z], \\ \partial_t S_{yz} + \frac{1}{3} \partial_y J_z &= \lambda [S_{yz} - \rho g(\rho) v_y v_z], \end{aligned} \quad (7)$$

where the  $z$  derivatives have been systematically dropped; we have deliberately omitted the propagation viscosity that results from second-order terms in the expansion of the streaming operator and which can be included by the simple rescaling  $1/\lambda \rightarrow 1/\lambda + \frac{1}{2}$  in the transport coefficients. In the adiabatic limit, by solving Eq. (7) for  $S_{xz}$  and  $S_{yz}$ , one obtains

$$\partial_t J_z + (\mathbf{v} \cdot \partial) J_z = -\frac{1}{3\lambda} \Delta J_z. \quad (8)$$

This is precisely Eq. (5) once  $J_z$  is identified with the stream function  $\phi$  and the diffusivity  $\chi$  with the coefficient  $-1/3\lambda$ . We now turn to the equation for  $\Delta \psi$ . Here the key observation is that the magnetic tension  $(\mathbf{B} \cdot \partial) \Delta \phi$  has exactly the same structure (up to a sign exchange) as the advection term  $(\mathbf{v} \cdot \partial) \Delta \psi$ . Since in Eqs. (3) the advection is given by the equilibrium expression of the stress tensor  $S_{\alpha\beta}^{\text{eq}}$ , it follows that, in order to model the magnetic tension, it is sufficient to extend the definition of the equilibrium distribution function as follows:

$$N_i^{\text{eq}} \rightarrow N_i^{\text{eq}} = d [1 + 2c_{i\alpha} v_\alpha + \rho G(\rho) Q_{i\alpha\beta} (v_\alpha v_\beta - B_\alpha B_\beta)]. \quad (9)$$

The equilibrium stress tensor now takes the following form:

$$S_{\alpha\beta}^{\text{eq}} = \rho g(\rho) \left[ v_\alpha v_\beta - B_\alpha B_\beta - \frac{v^2 - B^2}{4} \delta_{\alpha\beta} \right], \quad (10)$$

and, consequently, in the adiabatic limit, the equations for the velocity field become

$$\partial_t v_\alpha + (\mathbf{v} \cdot \partial) v_\alpha - (\mathbf{B} \cdot \partial) B_\alpha = \eta \Delta v_\alpha, \quad (11)$$

where  $\alpha = x, y$ . By using the definition of stream function, we finally obtain Eq. (6) with  $\eta = \chi = -1/3\lambda$ . This completes the proof that by removing the degeneracy along the  $z$  axis and modifying the equilibrium distribution function, it is possible to model the presence of a 2D magnetic field. Moreover, it should be noted that the present scheme can easily be extended to nonunit

“Prandtl” numbers  $\chi/\eta$ . For this purpose, one only needs to change the collision matrix by imposing two distinct eigenvalues  $\lambda_1$  and  $\lambda_2$  to the fields  $S_{xx}, S_{xy}, S_{yy}$  and  $S_{xz}, S_{yz}$ , respectively. By doing so, one has, in fact,  $\chi/\eta = \lambda_2/\lambda_1$ .

A few comments on our results are in order. The first point concerns computational efficiency: The LBE has been introduced to cope with the problem of statistical noise, which often affects Boolean LG simulations.<sup>9</sup> To this concern, it is useful to remember that the Reynolds number achievable in a LG simulation with  $N$  nodes per dimension is given by

$$N_{\text{Re}} = \frac{R^* MN}{h}, \quad (12)$$

where  $M$  is the sound Mach number  $M = U/c_s$ ,  $h$  the number of lattice sites needed to extract a single hydrodynamical variable, and  $R^*$  a dimensionless figure (of the order of the inverse mean free path in lattice units) that only depends on the collision rules. For a given value of the Reynolds number, the control-processing-unit (CPU) time needed by an  $N$ -step-long simulation is given by

$$t_{\text{CPU}} = \frac{N^3 N_{\text{op}}}{V}. \quad (13)$$

Here,  $N_{\text{op}}$  is the number of operations/site step and  $V$  is the processing speed of the given computer. For a given value of the Reynolds number we have

$$\frac{t_{\text{CPU}_{\text{LG}}}}{t_{\text{CPU}_{\text{LB}}}} = \left[ \frac{h_{\text{LG}}}{h_{\text{LB}}} \right]^3 \left[ \frac{R_{\text{LB}}^*}{R_{\text{LG}}^*} \right]^3 \left[ \frac{N_{\text{op, LG}}}{N_{\text{op, LB}}} \right] \left[ \frac{V_{\text{LG}}}{V_{\text{LB}}} \right]^{-1}. \quad (14)$$

For a 12-bit automaton, the most efficient implementation consists of performing the collision step by a single access of a precoded  $2^{12}$  12-bit- (6 kbyte) wide table lookup. The output state is simply read at the address given by the input state. Assuming that this access can be completed in the same number of machine cycles required by a single floating-point operation (flop), we can fix  $N_{\text{op, LG}} = 1$  and  $V_{\text{LG}} = V_{\text{LB}}$ . The MHD-LB scheme requires of the order of  $18^2/2 \sim 180$  flops/site. However, since only three distinct parameters occur in the collision matrix (its nonzero eigenvalues), these operations can be efficiently regrouped in such a way as to require no more than 100 effective flops. With these assumptions, Eq. (14) becomes

$$\frac{t_{\text{CPU}_{\text{LG}}}}{t_{\text{CPU}_{\text{LB}}}} = \left[ \frac{h_{\text{LG}}}{h_{\text{LB}}} \right]^3 \left[ \frac{R_{\text{LB}}^*}{R_{\text{LG}}^*} \right]^3 \frac{1}{100}. \quad (15)$$

Now, since the MHD-LB scheme is based upon the four-dimensional fchc algorithm, while the corresponding MHD automaton relies upon the two-dimensional FHP scheme, a ratio  $R_{\text{LB}}^*/R_{\text{LG}}^*$  of the order of 5 can be assumed. As a result, we obtain

$$\frac{t_{\text{CPU}_{\text{LG}}}}{t_{\text{CPU}_{\text{LB}}}} \simeq \left[ \frac{h_{\text{LG}}}{h_{\text{LB}}} \right]^3. \quad (16)$$

Previous numerical experience with both CA and LB schemes suggests  $h_{\text{LG}} \simeq \mathcal{O}(10)$  and  $h_{\text{LB}} \simeq \mathcal{O}(1)$ , which shows that the MHD-LB scheme is at least two orders of magnitude more efficient than the corresponding cellular automaton. A similar argument holds for computer storage, with a milder  $h^2$  factor. It is worth remembering, however, that noise elimination is achieved at the expense of exact Boolean computing, because, by the very fact of dealing with average quantities, the LBE scheme has to process rational and not binary numbers.

So much for the comparison between the LB method and the LG method. To get at least a qualitative appreciation of its absolute efficiency, the LB method should be compared with other floating-point techniques. Although a detailed comparison is beyond the scope of this paper, previous numerical experience of the authors<sup>10</sup> indicates that, for the case of two-dimensional incompressible turbulence, the LB method runs slightly faster than the pseudospectral method (probably the most well-established technique for homogeneous incompressible turbulence). However, independent of any consideration of actual performances, when put into a long-term perspective, two points seem to be definitely in favor of the LB technique: linear scalability (linear speed-up with the number of processors) for parallel computing and ease of implementation of complex boundary conditions.

At this stage, a few comments on the range of applicability of the LB-MHD scheme are appropriate. As is known, lattice gases need to be operated in a quasi-incompressible regime, with the sound Mach number  $M = U/c_s$  well below 0.2. In a MHD fluid, a further characteristic speed needs to be considered—that is, the

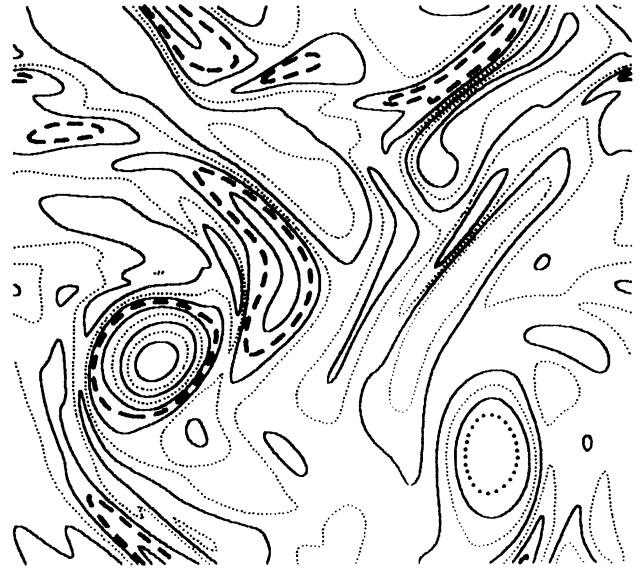


FIG. 1. Contour plots of the fluid vorticity. The simulation was performed on a  $128 \times 128$  grid. The presence of elongated structures is a clear signature of the vortex-stretching mechanism associated with the magnetic field.

Alfvén speed defined as  $c_A = B/\sqrt{\rho}$ , i.e., the typical propagation speed of magnetic perturbations. In view of the second-order expansion in the magnetic field in the expression of the equilibrium population, it is clear that our scheme is confined to small values of the Alfvén speed with respect to the sound speed, or, in terms of the current MHD terminology, to high values of the “beta” parameter, namely the ratio of thermal to magnetic pressure  $\beta = c_s^2/c_A^2 \gg 1$ . This is no surprise, since the above inequality is known to mark the domain where explicit methods (such as the one presented in this paper) can be applied. It should be noted that the dependence of the Alfvén speed on the inverse square root of the density is likely to sharpen the incompressibility constraint beyond the limits imposed to “conventional” lattice gases. As a result, the LB-MHD scheme proposed in this paper seems particularly suited to incompressible MHD flows in complex (i.e., porous) geometries.

Interesting applications may equally well be devised in the field of “conventional fluid dynamics,” for instance in the study of the statistical properties of 3D turbulence. In fact, it is known<sup>11</sup> that the magnetic tension mimics—in 2D—the effect of the vortex stretching term  $(\mathbf{v} \cdot \nabla)\text{rot}(\mathbf{v})$ , which plays a crucial role in the physics of fully developed turbulence. The presence of such a vortex-stretching term is clearly visible in Fig. 1, which shows a vorticity map on a  $128 \times 128$  grid.

#### ACKNOWLEDGMENTS

Two of us (M.V. and R.B.) thank the IBM European Center for Scientific and Engineering Computing (Rome), where the numerical simulations were performed on an IBM 3090 vector multiprocessor, for kind hospitality. We are grateful to U. Frisch and L. Pietronero for many stimulating hints and discussions.

<sup>1</sup>U. Frisch, D. d’Humières, B. Hasslacher, P. Lallemand, Y. Pomeau, and J. P. Rivet, *Complex Syst.* **1**, 649 (1987).

<sup>2</sup>U. Frisch, B. Hasslacher, and Y. Pomeau, *Phys. Rev. Lett.* **56**, 1505 (1986).

<sup>3</sup>D. d’Humières, P. Lallemand, and U. Frisch, *Europhys. Lett.* **2**, 291 (1986).

<sup>4</sup>D. Montgomery and G. Doolen, *Phys. Lett. A* **120**, 229 (1987).

<sup>5</sup>H. Chen and W. H. Matthaeus, *Phys. Rev. Lett.* **58**, 1845 (1987).

<sup>6</sup>F. Higuera and J. Jimenez, *Europhys. Lett.* **9**, 663 (1989).

<sup>7</sup>M. Vergassola, S. Succi, and R. Benzi, *Europhys. Lett.* **13**, 727 (1990).

<sup>8</sup>F. Higuera, S. Succi, and R. Benzi, *Europhys. Lett.* **9**, 345 (1989).

<sup>9</sup>S. Succi, P. Santangelo, and R. Benzi, *Phys. Rev. Lett.* **60**, 2738 (1988).

<sup>10</sup>R. Benzi and S. Succi, *J. Phys. A* **23**, L1 (1990).

<sup>11</sup>D. Biskamp and H. Welter, *Phys. Fluids B* **1**, 10 (1989).